Geophys. J. Int. (1993) **115,** 1161–1168

Thermal generation of ferromagnetic minerals from iron-enriched smectites

A. M. Hirt,[1] A. Banin[2] and A. U. Gehring[3]

[1] *Institut für Geophysik, ETH-Hönggerberg, 8093 Zürich, Switzerland*
[2] *Department of Soil and Water Sciences, The Hebrew University, Rehovot 76100, Israel*
[3] *Department of Soil Science, University of California, Berkeley, CA 94720, USA*

Accepted 1993 June 14. Received 1993 June 14; in original form 1993 February 3

SUMMARY

In recent years remagnetization of orogenic belts has been explained by fluid migration through rocks undergoing deformation. A laboratory study of remagnetization is presented in which varying amounts of iron (0–13.5 weight per cent Fe_2O_3) are adsorbed onto smectite surfaces. All smectite samples contain structural Fe (III) which is located in octahedral sites and is thermally stable up to 700 °C. An increase in the amount of iron adsorbed onto the clay surface leads to the formation of ferric nanophases in which parts are magnetic. Mineralogical changes that occur during thermal treatment between room temperature and 700 °C were monitored using electron spin resonance (ESR), bulk susceptibility, acquisition of isothermal remanent magnetization (IRM) and Curie temperature analysis. After heating the samples to 250 °C, a new ferrimagnetic phase is created as indicated by ESR and IRM acquisition. ESR spectra, IRM acquisition and Curie analyses suggest that magnetite is the predominant phase that is being created. These grains continue to be created and grow with heating up to 500 °C. Above this temperature a decrease in the intensity of the IRM at 1T suggests that the phase is being transformed into haematite. The thermal experiments on iron-loaded smectites show that surface-induced processes can lead to the formation of new magnetic minerals under conditions characteristic of low-grade metamorphism.

Key words: magnetite, mineralogy, remanent magnetization.

INTRODUCTION

Remagnetization is often prevalent in areas that have undergone tectonic deformation. Traditionally, a thermoviscous mechanism has been invoked in order to explain the remagnetization of pre-existing ferrimagnetic minerals (*cf.* Pullaiah *et al.* 1975; Kent 1985). For several years, remagnetization has been attributed to the precipitation of new ferromagnetic minerals during fluid migration associated with the mountain-building process (Oliver 1986; Miller & Kent 1988; McCabe & Elmore 1989; McCabe, Jackson & Saffer 1989; Bethke & Marshak 1990). Such processes have been applied to the Appalachian fold belt where fine-grained magnetite generally carries the remagnetized component in carbonates (McCabe *et al.* 1983; Jackson 1990). Several studies have deduced a relationship between degree of illitization, potassium feldspar content and the magnetite content in remagnetized limestones from the Appalachian plateau in New York State (Jackson *et al.* 1988; Lu *et al.* 1991; Saffer & McCabe 1992). In this model remagnetization is explained by induced pulses of heated fluids which pass through the basin and trigger the growth of magnetite when iron is released from iron-bearing smectites during illitization.

Sheet silicates such as smectites and illites have reactive surfaces which favour adsorption processes (Goldberg 1989). Such processes play an important role in the mobilization and precipitation of ions in natural systems (e.g. Stumm & Morgan 1981). Electron spin resonance (ESR) studies have shown that iron as nanophases (phases of nanometer grain size) associated with reactive surface sites, apart from structural Fe (III), can occur in smectites (Goodman 1978; Craciun & Maghea 1985). Annealing experiments have demonstrated that iron-enriched smectites are metastable and lead to the formation of ferric oxides (Luca & Cardile 1989). However, the role of surface-induced processes during the magnetization of rocks under elevated temperature has not been studied thus far.

The purpose of this study is to present experimental data of the formation of magnetic phases on the surface of

smectite in order to explain the magnetization under burial or low metamorphic conditions.

MATERIALS AND METHODS

A smectite (SWj-1) clay, a Na-montmorillonite, from Crook County, Wyoming, was obtained from the Clay Mineral Society Repository. A comprehensive summary of the chemical and mineralogical properties of this Na-montmorillonite has been published by van Olphen & Fripiat (1979). Its chemical formula can be described as $M_x[Si_8]Al_{3.2}Fe_{0.2}Mg_{0.6}O_{20}(OH)_4$, where M_x is the monovalent interlayer cation Na^+ and x is the layer charge (0.5–1.2 for smectite). The ionic composition of the parent clay, which was supplied in powder form, was converted using the 'quantitative ion exchange method' (QIEM) (Banin 1973; Gerstl & Banin 1980). This method entails titrating a mixture of freshly prepared hydrogen-saturated montmorillonite and OH-saturated ion-exchange resin in suspension, with the chloride salt in the desired exchangeable cation. Nitrogen gas was bubbled in the suspension during titration to displace oxygen and prevent, or slow down, the oxidation of Fe^{2+} in solution. The procedure was conducted starting with a batch (~200 g) of hydrogen clay. The clay was titrated at a constant rate with a 1 N $FeCl_2$ solution in the presence of excess, strongly basic OH-anion exchange resin (Aberilite IR-410). The pH and electrical conductivity were monitored continuously during the titration. Aliquots of the clay suspensions were withdrawn from the batch after predetermined amounts of iron were added. The Eh was measured using a Pt/calomel electrode pair. The clay-iron preparations were then centrifuged, freeze-dried, and lightly crushed to pass a mesh of 0.105 mm. The powders were stored at room temperature for further analyses. The specific surface areas of the samples were measured by the EGME adsorption method (Ratner-Zohar, Banin & Chen 1983).

The parent smectite sample (AB01) has a light greyish colour (Munsell colour charts: 7.5YR8/0) and the iron-loaded samples become increasingly orange to reddish-brownish (7.5YR7/4 to 5YR6/8). The adsorbed 'iron' is a mixture of Fe(III)/Fe(II) and iron oxide/iron oxyhydroxide of poor crystallinity. Oxidation of the Fe(II) takes place during the titration and then (mostly) during the freeze-drying step. Fe(III) is the predominant form of iron at loadings below the CEC (critical exchange capacity) of the clay, and the oxide/oxyhydroxide is predominant at loadings above the CEC of the clay.

The samples were identified by powder X-ray diffractometry (XRD) with a Gunier IV camera (model TR552, Enaf Nonius, Delft), using Cu–Kα radiation. ESR spectroscopic analyses were performed on untreated samples and samples that were heated stepwise between 100 and 700 °C in an oven for 12 hr at each step. ESR spectra were recorded on a Bruker 200ER spectrometer operating at X-band frequency with a 100 kHz magnetic field modulation and equipped with an Oxford Instruments ESR-900 cryostat. The spectrometer settings were 0.1 mT modulation amplitude, and a 2 mW microwave source with a 9.38 GHz frequency. The ESR spectra were recorded at room temperature and at 7 K, and processed to determine g-values (N,N-diphenylpicrylhydrazyl as reference for g-values) and hyperfine-coupling constants using computer-scope programs from R.C. Electronics (Santa Barbara, California).

The acquisition of isothermal remanent magnetization (IRM), bulk susceptibility, and intensity of the saturation IRM (SIRM) were measured on untreated samples and samples that were heated incrementally in a Schonstedt thermal demagnetizer to 700 °C for 90 min at each step. They were cooled to room temperature and then measured, before heating for a further increment of time. The IRM of the untreated and the heated samples was measured on a three-axis, 2G-Cryogenic magnetometer with a lower sensitivity of $4\,Am^2\,kg^{-1}$. An IRM was imparted to the powder samples, packed into a hole drilled into a plexiglass cylinder with a 2.5 cm diameter, by an electromagnet. The plexiglass holder also acquired an IRM, which was weak and removable by demagnetizing it in an alternating field of 100 mT. IRM acquisition of the holder after demagnetization was repeatable, where a magnetization of similar intensity was acquired after application of each new field. This signal was then subtracted from the IRM intensity of the holder with a sample. The bulk susceptibility was measured on a KLY-2 Susceptibility Bridge with a sensitivity of 4×10^{-8} (SI).

Curie temperature analysis was performed on the powder samples in a 0.2 T field, using a horizontal motion Curie balance (Lebel 1985), in order to trace the creation or change in the ferrimagnetic mineralogy of the smectites.

RESULTS

Mineralogical and spectroscopic analyses

The smectite sample (AB01) that had no iron loaded on its surface has a specific surface area (SSA) value of $829 \pm 0.5\,m^3\,g^{-1}$. No significant change in the SSA values was observed with the increased addition of iron (Table 1). X-ray diffraction of the iron-loaded samples showed no detectable peaks for ferric oxides. This suggests that the loaded iron forms a mixture of Fe–oxides/hydroxides, containing mainly Fe(III) and probably Fe(II).

The ESR spectra of the samples exhibits a low-field and high-field resonance around $g = 4.3$ and $g = 2$, respectively (Fig. 1). The signal around $g = 4.3$ is typical for high-spin Fe(III) in a strongly orthorhombic crystal field and can be attributed to Fe(III) in the octahedral sites of the smectites

Table 1. Weight per cent Fe_2O_3 and specific surface area for smectite samples

Sample	Total weight per cent Fe_2O_3*	Loaded weight per cent Fe_2O_3	Specific surface area ($m^2\,g^{-1}$)
AB01	2.78	0.00	829 ± 0.5
AB09	7.33	4.55	814 ± 12.3
AB13	9.31	6.53	774 ± 3.9
AB15	9.68	6.90	801 ± 10.0
AB16	9.45	6.67	859 ± 14.2
AB20	13.5	10.7	—

* Air dry basis.

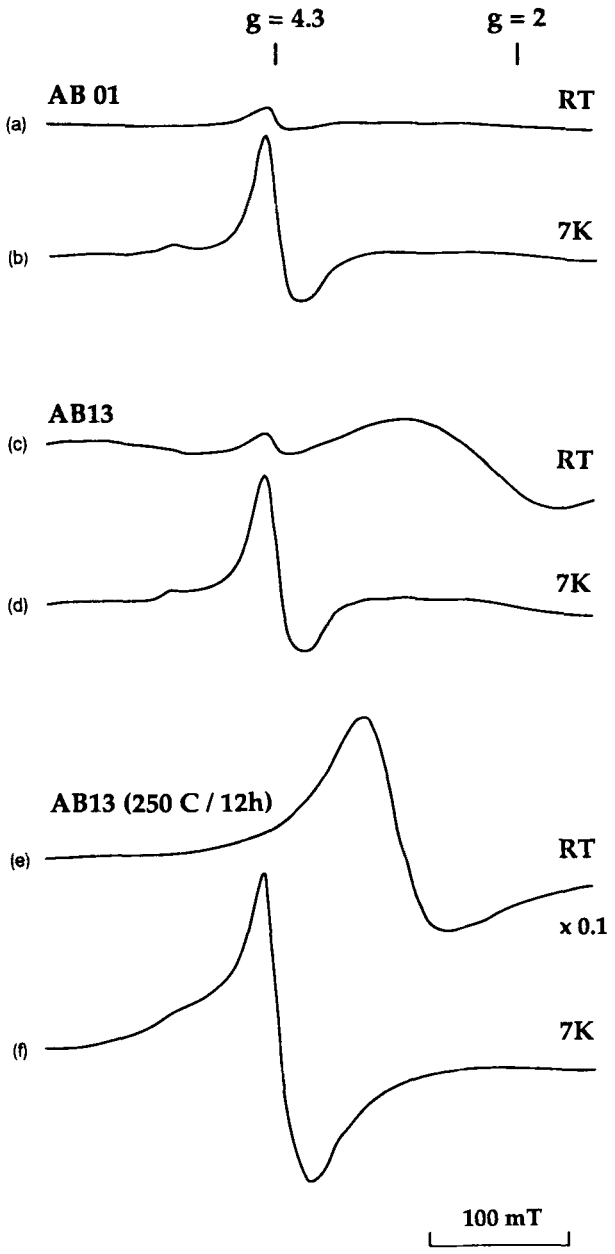

Figure 1. ESR spectra of a parent smectite (AB01) and a smectite with 6.5 weight per cent Fe_2O_3 adsorbed onto the surface (AB13). (a) Unheated AB01 measured at room temperature (RT); (b) AB01 after being heated to 250 °C and measured at 7 K; (c) unheated AB13 measured at RT; (d) unheated AB13 measured at 7 K; (e) AB13 after being heated to 250°C and measured at room temperature; (d) AB13 after being heated to 250 °C and measured at 7 K.

(e.g. Meads & Malden 1975). Room temperature spectra of iron-loaded samples reveal an additional broad signal around $g = 2$ (Fig. 1). The intensity of this signal increases with an increase in the iron added to the smectite surface. The broad lineshape of the $g = 2$ signal is mainly caused by electron spin–spin interaction between the Fe(III) ions at the smectite surface (Coyne & Banin 1986). Low-temperature measurements at 7 K result in a drastic increase of the signal intensity.

Upon stepwise heating up to 700 °C the low- and the high-field resonance show a different behaviour. The $g = 4.3$ signal which is assigned to structural Fe(III) located in octahedral sites of the smectite remains stable with heating. The $g = 2$ signal which is attributed to adsorbed Fe(III) is thermally stable up to 200 °C. Further annealing to 250 °C leads to a drastic increase of the intensity for all the iron-loaded samples. The most marked increase is observed for sample AB13 (Fig. 1). The newly formed intense signal shows a g-value around 2.6 and a peak-to-peak linewidth of 65 mT. Upon cooling down to 7 K the signal intensity decreased and only a very weak signal was measured, superimposed on the $g = 4.3$ signal. The signal intensity, the thermal behaviour and the shift of the g-value to lower fields is characteristic for ferrimagnetic resonance (FMR) and indicates either the formation of maghemite or magnetite (Griscom 1984; Gehring, Karthein & Reller 1990; Hirt & Gehring 1991). No significant changes of the ESR spectra were observed with further heating to 700 °C.

Rock magnetic analyses

IRM acquisition

The acquisition of IRM of the powders indicates that a low coercivity ferrimagnetic mineral is present in all samples, including the parent smectite powder (Fig. 2). Saturation occurs between 100 and 150 mT. Reverse field demagnetization was done in order to obtain an estimate of the coercivity of remanence (H_{cr}). H_{cr} values were between 18 and 24 mT for all samples, except the parent smectite which has a H_{cr} of 32 mT. The relationship between the intensity of the saturation IRM and total iron content of the sample is shown in Fig. 3. With increasing iron the saturation IRM also increases, which suggests the presence of more ferrimagnetic material as more iron has been adsorbed onto the surface. Fig. 4 shows an example of the IRM acquisition for sample AB13 after each heating step. The IRM acquisition can be differentiated into three types of behaviour with progressive heating. The samples show a small decrease in the SIRM when heated between room temperature and 200 °C, and H_{cr} remains around 20 mT

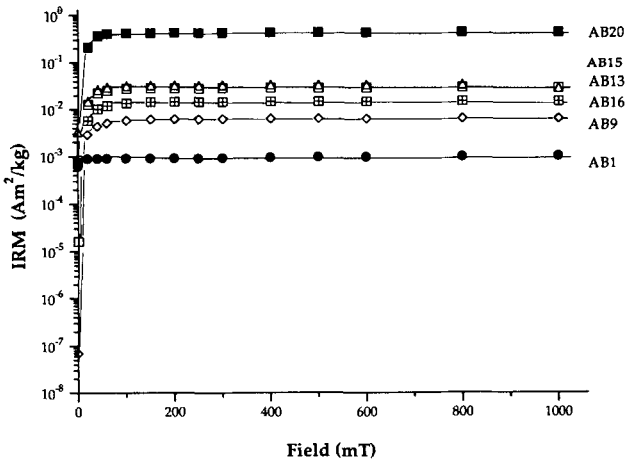

Figure 2. Progressive acquisition of IRM of all samples in an increasing magnetic field.

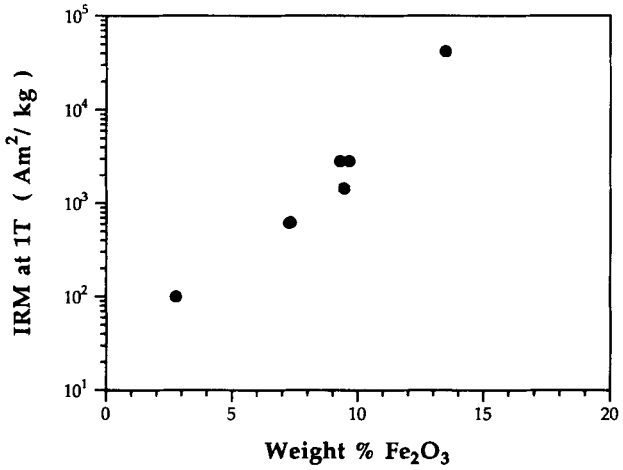

Figure 3. Variation of the SIRM with total weight per cent.

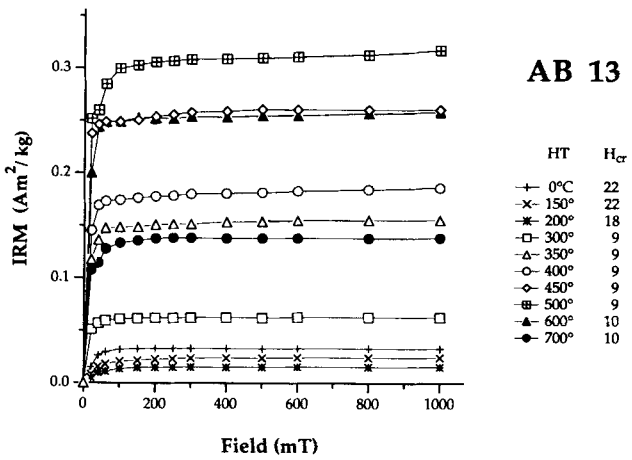

Figure 4. Progressive acquisition of IRM for a representative sample in an increasing magnetic field, after heating to the indicated heating temperature (HT). H_{cr} is the remanent coercivity of the IRM.

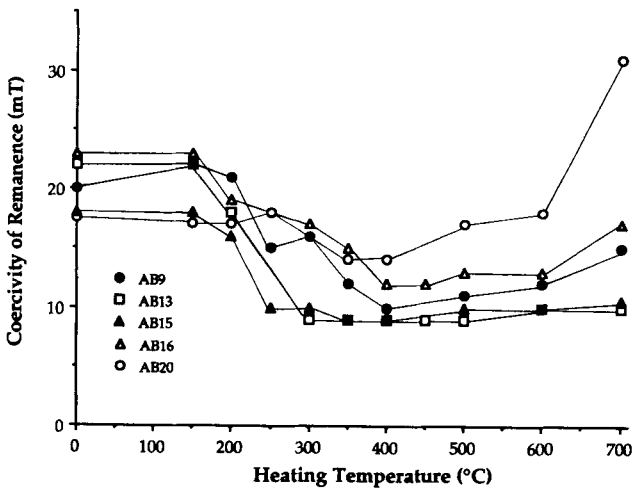

Figure 5. Change in H_{cr} with heating temperature (HT) for all samples.

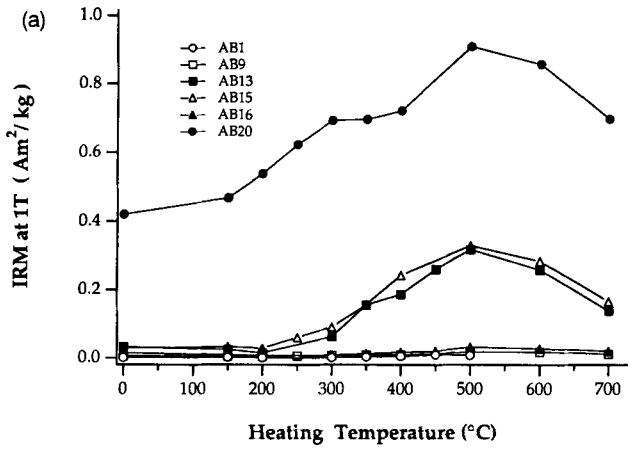

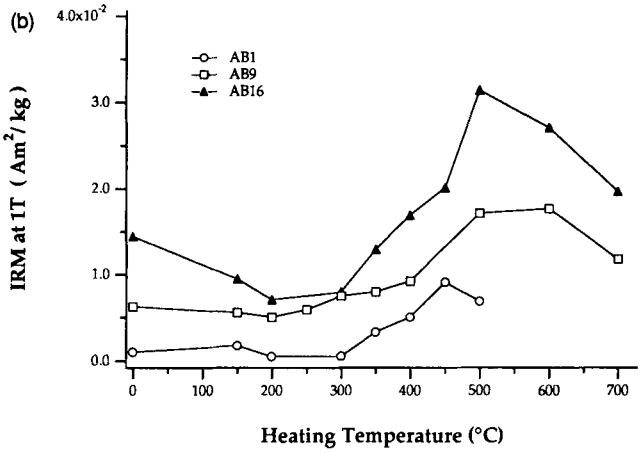

Figure 6. (a) Change in the IRM at 1 T with heating temperature (HT) for all samples. (b) Change in the IRM at 1 T with HT for samples AB 1, 9, and 16.

(Fig. 5). Heating the smectites above 200 °C to 500 °C, results in a progressive increase in the IRM acquired at 1 T, where near saturation is reached at approximately 200 mT (Fig. 4). The H_{cr} decreases after heating above 200 °C to 10 mT (Fig. 5). Further heating of the samples above 500 °C shows a drop in intensity of the IRM at 1 T and, for this sample, a slight increase in H_{cr}. The IRM behaviour of all the samples during heating is summarized in Fig. 6. The smectite samples AB9, 15, and 16 behave as described above.

The parent smectite also contains a ferrimagnetic component which is probably due to contamination. There is little change in the IRM acquired at 1 T until 350 °C with the IRM saturating between 100 and 150 mT. A new ferrimagnetic mineral starts to be created upon heating to 350 °C and above (Fig. 6). The IRM acquisition curve is still dominated by a low coercivity phase, but the sample is no longer near saturation at 1 T. An increase in the IRM intensity peaks at 450 °C, followed by a decrease after heating to 500 °C. Due to the weak intensity of this sample it was not possible to make an accurate determination of H_{cr}.

Sample AB20 behaves differently in that there is an

increase in the IRM at 1 T after the first heating step at 150 °C (Fig. 6). The intensity continues to increase upon further heating up to 500 °C. Heating above this temperature leads to a drop in the intensity of the IRM at 1 T. From Fig. 5 it is clear that the drop in intensity is associated with the creation of a higher coercivity mineral.

IRM acquisition at low temperature

The relation between the IRM intensity and temperature was investigated for selected samples (AB9, 15, 20) after they had been heated to 700 °C. A sample was given an IRM at 1 T at room temperature and subsequently cooled in liquid nitrogen; the magnetization was then remeasured for the cooled sample. A 10–30 per cent decrease in the intensity of the magnetization was observed. Samples were again cooled in liquid nitrogen, given an IRM and immediately measured. The intensity of the SIRM at liquid nitrogen temperature was up to six times higher than that observed at room temperature. After the samples warmed up to room temperature, they show a 50–75 per cent drop in the intensity of the SIRM compared to that measured at liquid nitrogen temperature.

Bulk susceptibility and SIRM intensity

Two samples of AB13 were heated to 150 °C and 250 °C, respectively, for increasing periods of time and the change in the bulk susceptibility and SIRM intensity were observed to monitor the effect of heating time on the growth of ferrimagnetic minerals. The sample heated at 150 °C showed little change in the SIRM intensity after heating for the first 1000 min (Fig. 7a). The bulk susceptibility showed a steady decline up until 600 min cumulative heating time. The second sample was heated at 250 °C, and for the first 10 min only a slight decrease in both the SIRM intensity and the bulk susceptibility was noted (Fig. 7b). Further heating led first to an increase in the bulk susceptibility, and later to an increase in the SIRM intensity. The bulk susceptibility continued to increase in intensity for the first several hundred minutes of cumulative heating. Afterwards, except for minor fluctuations, the intensity remained around 24 $m^3 kg^{-1}$. The increase in the SIRM intensity lagged behind the change in the bulk susceptibility, but continued to increase until 3000 min of cumulative heating.

Curie temperature analysis

The thermomagnetic curves show a linear decay from room temperature until approximately 250 °C, at which point the magnetization starts to increase until approximately 280 °C, indicative of the creation of a new ferrimagnetic phase (Fig. 8). The linear decay then continues until approximately 590–600 °C. Upon cooling, a magnetization is induced which increases down to room temperature. Reheating the same sample a second time produces a heating and cooling curve that is nearly identical to the cooling curve from the first heating. This behaviour suggests that the newly created ferrimagnetic phase with a Curie temperature of about 560 °C is thermally stable. The linear style decay is typical for samples that contain a large superparamagnetic fraction.

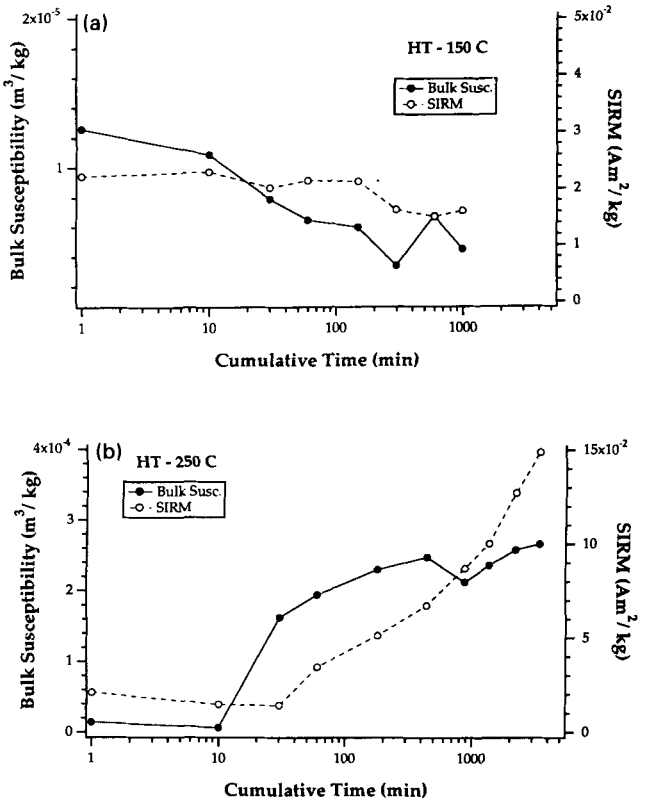

Figure 7. (a) Change of bulk susceptibility and SIRM with cumulative heating at 150°C for AB13. (b) Change of bulk susceptibility and SIRM with cumulative heating at 250°C for AB13.

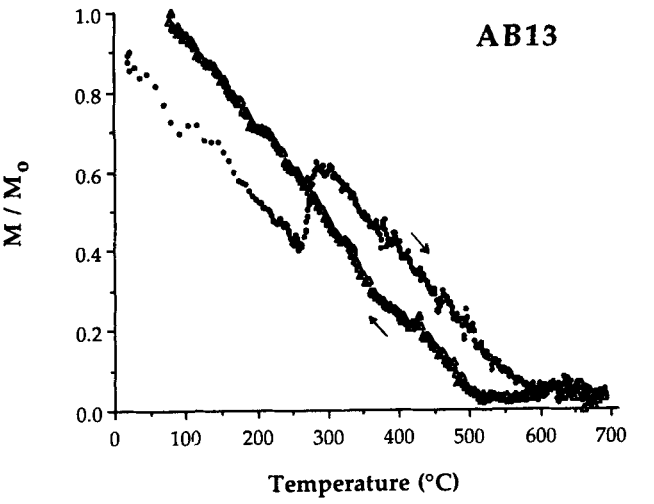

Figure 8. Thermal dependence of the magnetization induced in a 0.2 T field for AB13. A heating and cooling rate of 12 °C/min was used.

DISCUSSION

The experiments in the laboratory on iron-enriched smectites simulate the natural reaction sequences of hydrolysis–precipitation–oxidation during weathering of iron-containing primary silicate rocks and thermal conversion of weathering products under metamorphic conditions.

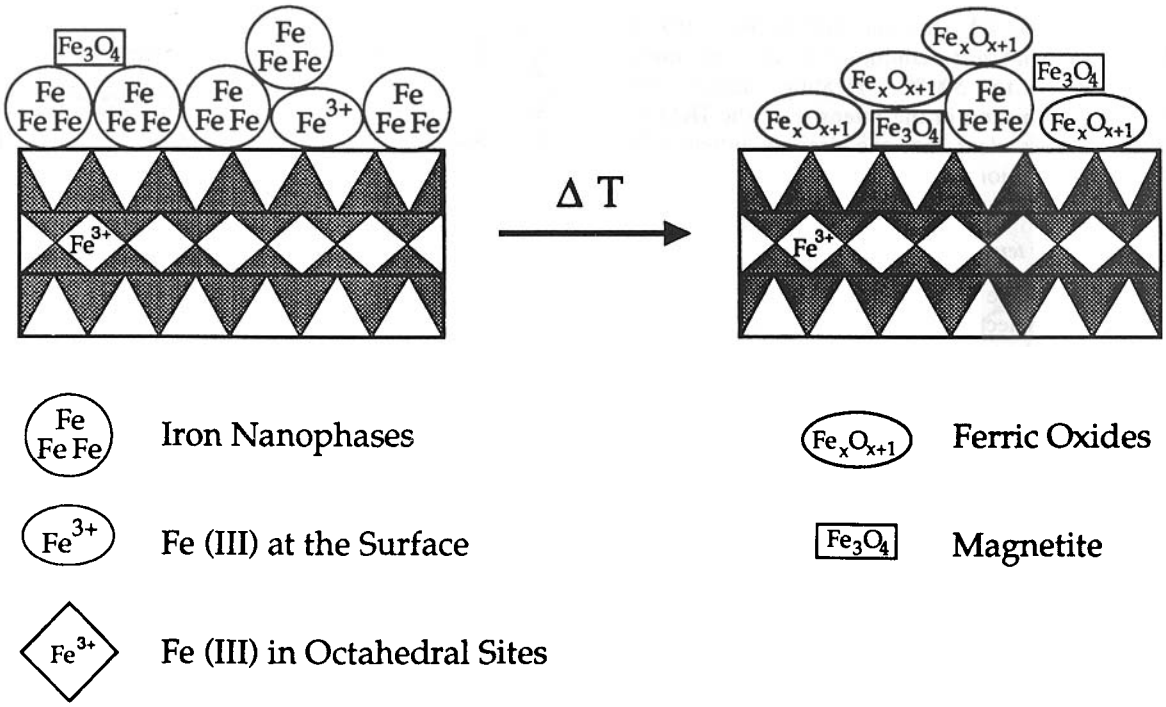

Figure 9. Schematic diagram of smectite in which Fe(III) has been loaded onto the surface before heating; and after heating.

The magnetic results clearly indicate that the parent sample contains a low coercivity ferrimagnetic mineral from the start. In addition, all samples contain structural Fe(III) located in octahedral sites of the smectites (Fig. 9).

The procedure used to load iron onto the smectite surfaces may lead to the initial formation of green-rust which is generally unstable and which oxidizes to other nanophase ferric oxides which are X-ray amorphous. This suggests that the clay acts as an effective matrix, both chemically and sterically, which prevents the major part of the synthesized iron oxides from ripering, i.e. growing to larger cystals. The correlation between the amount of ferrimagnetic phases and the amount of adsorbed iron indicates that the clay surface can act as a catalyst for the formation of very fine-grained ferric oxides (magnetite and/or maghemite).

The acquisition of IRM and thermomagnetic curves and ESR suggest that the extractable iron on smectite surfaces is thermally stable up to 200 °C, except for sample AB20 which has a higher iron content and is less stable (Fig. 3). Heating above 200 °C leads to the creation of a ferrimagnetic phase. This phase is magnetite and/or maghemite as indicated by the FMR signal. The thermal stability of the $g = 4.3$ ESR signal, arising from Fe(III) in octahedral sites of the smectite, suggests clearly that structural iron is not involved in the formation of the magnetic phases (Fig. 2). Therefore, it can be postulated that the magnetic phases were formed due to the conversion of the Fe(III) phases at the smectite surface. In the cumulative heating experiments at 250 °C the increase of the bulk susceptibility before the SIRM (Fig. 7) indicates the formation of grains whose volumes are in the super-paramagnetic grain size range. With further heating, these grains grow larger and are able to retain a remanent magnetization. By increasing the time of heating, more magnetite/maghemite is generated and this grows from superparamagnetic to single domain grain size, and eventually to multi-domain size. The IRM imparted at low temperature yields a significantly stronger magnetization than that given at room temperature which implies the presence of grains of superparamagnetic size. By heating the iron-rich smectites to higher temperatures the reactions are probably driven faster; therefore, there is an increase in intensity of the IRM at 1 T with each heating step. Heating to temperatures above 500 °C shows a decrease in the IRM intensity which can be interpreted in terms of a conversion of magnetite/maghemite to haematite. The conversion of magnetite to haematite above 500 °C has often been observed during thermal treatment of limestones (Lowrie & Heller 1982).

Since the precursor of the magnetic mineral which forms during heating is amorphous and not well characterized, the question remains as to the identification of this low coercivity phase. Several earlier studies that examined changes in the magnetic behaviour of nontronite, another iron-rich smectite, also found the creation of a ferrimagnetic phase with heating (Geilmann, Klemm & Meisel 1932; Moskowitz & Hargraves 1982, 1984). Gielmann *et al.* (1932) noted that heating a nontronite powder led to: (1) a slight decrease in magnetic susceptibility between 300 and 400 °C associated with the release of structural water; (2) an increase in the susceptibilty after heating to 800–1000 °C; and (3) a decrease in susceptibility above 1000 °C. The increase in susceptibility above 800 °C was attributed to the growth of maghemite (γ-Fe_2O_3), and the decrease above 1000 °C was due to the conversion of γ-Fe_2O_3 to α-Fe_2O_3 (haematite).

Moskowitz & Hargraves (1984) heated nontronite powders for 60 min intervals between 100 and 700 °C, but found no generation of a ferrimagnetic phase. Only after annealing their samples at temperatures of 700 °C or

greater, were they able to generate a ferrimagnetic phase. Annealing the sample at 900 °C for 5 min led to the creation of a low coercivity mineral. Heating for longer periods of time showed a conversion of the low coercivity phase into a higher coercivity phase, which the authors considered to be γ-Fe_2O_3 converting to α-Fe_2O_3. It should be noted that all of their examples, including the sample heated for 5 min displayed IRM acquisitions that were not saturated in a field of 1 T.

In contrast to the iron-loaded montmorillonite in this study, the iron in nontronite is lattice bound. The ferrimagnetic phase was only generated above 700 °C after the clay structure started to break down. It has also been reported that maghemite synthesized at high temperatures (above 650 °C) and/or high pressures can be stable in a similar temperature range to magnetite (*cf.* Renshaw & Roscoe 1969). In contrast, maghemite formed by thermal conversion of a hydroxide precursor under ambient pressure—the situation found at the clay surface—is thermally less stable and converts to haematite by 450 °C (e.g. Verwey 1935; Gómez-Willacieros *et al.* 1984; Gehring & Hofmeister 1992).

The iron-loaded samples reported on in this study all showed an IRM acquisition that is saturated by 200 mT. The new magnetic phase forms from a precursor phase under ambient pressure and temperatures less than 600 °C. If maghemite were the predominant phase, some maghemite should oxidize to haematite before heating above 500 °C (Gómez-Villacieros *et al.* 1984; Gehring & Hofmeister 1992). The thermal stability of this newly formed phase at the smectite surface suggests that magnetite is the predominant mineral that is being formed and controls the magnetic properties of the samples.

The only exception that is observed is for the parent smectite (not iron loaded). It showed the generation of a ferrimagnetic phase only after heating to 350 °C or above. Both a high and low coercivity component were seen in the IRM acquisition. Further heating always led to an increase of the high coercivity component, suggesting that maghemite was the original low coercivity mineral being created in the parent clay.

The above data demonstrate that iron can be adsorbed onto clay minerals and can form amorphous and fully crystallized oxides and/or hydroxide phases. These adsorption processes can occur under diagenetic and low metamorphic conditions when fluids interact with clay minerals (Fig. 9). The magnetic analyses clearly show that such a process can also lead to the formation of magnetic nanophases at room temperature. The thermally induced magnetization of the iron-enriched clay occurs between 200 and 250 °C, a metamorphic temperature range that is assumed for several orogenic belts. The formation of magnetite can be explained by a simple conversion of adsorbed ferric precursors. Since the ESR spectra with g-value = 4.3 are not affected by the thermal treatment, the structural Fe(III) in the octahedral sites is not involved in the formation of the magnetic phases.

Models for remagnetization in orogenic belts (e.g. Appalachian and Asturian fold–thrust belts) include thermoviscous remagnetization or chemical remagnetization. Although a thermoviscous remagnetization is possible in the easternmost part of the Appalachian fold and thrust belt, it is difficult to invoke this model for the western part of the fold belt or in the mid-continent since temperatures never exceed 150–200 °C (Epstein, Epstein & Harris 1977; McCabe & Elmore 1989). Since the thermoviscous model cannot satisfy remagnetization on a large scale in the Appalachian orogen, illitization of smectite linked with precipitation of magnetite has been proposed as a key mechanism for chemical remagnetization (McCabe & Elmore 1989). This model assumes that iron used to create the magnetite is released from the smectite structure. Illitization of smectite is controlled by multiple kinetic factors, i.e. temperature, time, activation of chemical components and the rock/water ratio (Weaver 1988; and references therein), and such a process is very difficult to deduce in rocks when only the products are preserved. For the illitization model in the Appalachian fold belt, for example, the precursor iron-bearing smectite cannot be identified directly (Lu *et al.* 1991).

This laboratory study on iron-loaded smectite does not preclude that the above processes can also lead to the formation of magnetite. These results, however, offer a simple thermal-induced mechanism in order to explain a chemical remanent magnetization of rocks under burial or low metamorphic conditions.

CONCLUSIONS

The experimental study has shown that iron adsorbed onto the surface of smectites can lead to iron nanophases. These phases are X-ray amorphous but part of them are magnetic. If these ferric nanophases are heated to temperatures above 250 °C, they convert to new ferrimagnetic minerals. The conversion to a magnetic phase increases with higher temperature and longer heating time. Magnetite is the predominant phase formed, controlling the magnetic properties of the iron-loaded smectites. The formation of magnetic phases up to 700 °C involves only the iron adsorbed onto the surface. These experimental data can be used to explain remagnetization of sedimentary rocks under low-grade metamorphic conditions.

ACKNOWLEDGMENTS

The authors are grateful to I. V. Fry for providing the ESR analyses. W. Lowrie, W. Hirt and two anonymous reviewers are thanked for critically reading the manuscript. This research was supported by the Swiss National Science Foundation, project no. 20-28884.90 (A.M. Hirt), and project no. 8220-08438. (A.U. Gehring). ETH-Contribution no. 758.

REFERENCES

Banin, A., 1973. *Quantitative ion exchange process for clays,* US Patent No. 3 725 528.

Bethke, C. M. & Marshak, S., 1990. Brine migration across North America—the plate tectonics of groundwater, *Ann. Rev. Earth planet. Sci.*, **18,** 287–315.

Coyne, L. M. & Banin, A., 1986. Effect of adsorbed iron on thermoluminence and electron spin resonance spectra of Ca–Fe exchanged montmorillonite, *Clays Clay Mineral.*, **34,** 645–650.

Craciun, C. & Maghea, A., 1985. Electron spin resonance studies of montmorillonites, *Clay Miner.*, **20,** 281–290.

Epstein, A. G., Epstein, J. B. & Harris, L. D., 1977. Conodont color alteration—an index to organic metamorphism, *U.S. Geol. Sur. Prof. Pap.*, **995,** 1–27.

Gehring, A. U. & Hofmeister, A., 1992. Magnetic and spectroscopic study of the γ-FeOOH–γ-Fe_2O_3–α-Fe_2O_3-system, *EOS, Trans. Am. geophys. Un.*, **73,** 98.

Gehring, A. U., Karthein, R. & Reller, A., 1990. Activated state in the lepidocrocite structure during thermal treatment, *Naturwiss.*, **77,** 177–179.

Geilmann, W., Klemm, W. & Meisel, K., 1932. Das Auftreten hochmagnetischer Zwischenstufen bei der thermische Zersetzung des Nontronits, *Naturwiss.*, **20,** 639–640.

Gerstl, Z. & Banin, A., 1980. Fe^{2+}–Fe^{3+} transformations in clay and resin ion-exchange systems, *Clays Clay Mineral.*, **28,** 335–345.

Goldberg, S., 1989. Interaction of aluminium and iron oxides and clay minerals and their effect on soil physical properties: a review, *Commun. Soil Sci. Plant Anal.*, **20,** 1181–1207.

Gómez-Willacieros, R., Hernán, L., Morales, J. & Tirado, J. L., 1984. Textural evolution of synthetic γ-FeOOH during thermal treatment by different scanning calorimetry, *J. Coll. Interf. Sci.*, **101,** 392–400.

Goodman, B. A., 1978. An investigation by Mössbauer and EPR spectroscopy of the possible presence of iron-rich impurity phases in some montmorillonites, *Clay Miner.*, **13,** 351–356.

Griscom, D. L., 1984. Ferromagnetic resonance of precipitated phases in natural glasses, *Non cryst. Solids*, **67,** 81–118.

Hirt, A. M. & Gehring, A. U., 1991. Thermal alteration of the magnetic mineralogy in ferruginous rocks, *J. geophys. Res.*, **96,** 9947–9953.

Jackson, M., 1990. Diagenetic sources of stable remanence in remagnetized Paleozoic cratonic carbonates: a rock magnetic study, *J. geophys. Res.*, **95,** 2753–2761.

Jackson, M., McCabe, C., Ballard, M. M. & Van der Voo, R., 1988. Magnetite authigenesis and diagenetic paleotemperatures across the northern Appalachian basin, *Geology*, **16,** 592–595.

Kent, D. V., 1985. Thermoviscous remagnetization in some Appalachian limestones, *Geophys. Res. Lett.*, **12,** 805–808.

Lebel, P., 1985. Inbetriebnahme und Verwendung einer Curiewaage, *Diploma thesis*, ETH-Zürich.

Lowrie, W. & Heller, F., 1982. Magnetic properties of marine limestones, *Rev. Geophys. Space Phys.*, **20,** 171–192.

Lu, G., McCabe, C., Hanor, J. S. & Ferrell, R. E., 1991. A genetic link between remagnetization and potassic metasomatism in the Devonian Onondaga formation, Northern Appalachian basin, *Geophys. Res. Lett.*, **18,** 2047–2050.

Luca, A. & Cardile, C. M., 1989. Cation migration in smectite minerals: electron spin resonance of exchanged Fe^{3+} probes, *Clays Clay Mineral.*, **37,** 325–332.

McCabe, C. & Elmore, R. D., 1989. The occurrence and origin of the late Paleozoic remagnetization in sedimentary rocks, *Rev. Geophys.*, **27,** 471–494.

McCabe, C., Van der Voo, R., Peacor, D. R., Scotese, C. R. & Freeman, R., 1983. Diagenetic magnetite carries ancient yet secondary remanence in some Paleozoic sedimentary carbonates, *Geology*, **11,** 221–223.

McCabe, C., Jackson, M. & Saffer, B., 1989. Regional patterns of magnetic authigenesis in the Appalachian basin: Implications for the mechanism of Late Paleozoic remagnetization, *J. geophys. Res.*, **94,** 10 492–10 443.

Meads, R. E. & Malden, P. J., 1975. Electron spin resonance in natural kaolinites containing Fe^{3+} and other transition metal ions, *Clay Miner.*, **10,** 313–345.

Miller, J. D. & Kent, D. V., 1988. Regional trends in the timing of Alleghanian remagnetization in the Appalachians, *Geology*, **16,** 588–591.

Moskowitz, B. M. & Hargraves, R. B., 1982. Magnetic changes accompanying the thermal decomposition of nontronite (in air) and its relevance to Martian mineralogy, *J. geophys. Res.*, **87,** 10 115–10 128.

Moskowitz, B. M. & Hargraves, R. B., 1984. Magnetic Cristobalite (?): a possible new magnetic phase produced by thermal decomposition of nontronite, *Science*, **225,** 1152–1154.

Oliver, J., 1986. Fluids expelled tectonically from orogenic belts: their role in hydrocarbon migration and other geologic phenomena, *Geology*, **14,** 99–102.

Pullaiah, G., Irving, E., Buchan, K. L. & Dunlop, D. J., 1975. Magnetization changes caused by burial and uplift, *Earth planet. Sci. Lett.*, **28,** 133–143.

Ratner-Zohar, Y., Banin, A. & Chen, Y., 1983. Oven drying as a pretreatment for surface area determinations of solids and clays, *Soil Sci. Soc. Am. J.*, **7,** 1056–1057.

Renshaw, G. D. & Roscoe, C., 1969. Thermal stability of γ-ferric oxide, *Nature*, **224,** 263–264.

Saffer, B. & McCabe, C., 1992. Further studies of carbonate remagnetization in the Northern Appalachian basin, *J. geophys. Res.*, **97,** 4331–4348.

Stumm, W. & Morgan, J. J., 1981. *Aquatic Chemistry*, Wiley, New York.

van Olphen, H. & Fripiat, J. J., 1979. *Data Handbook for Clays and Other Nonmetallic Materials*, Pergamon Press, Oxford.

Verwey, E. J. M., 1935. The crystal structure of γ-Fe_2O_3 and γ-Al_2O_3, *Z. Kristallogr.*, **91,** 65–69.

Weaver, C. E., 1988. Clays, mud and shales, *Developments in Sedimentology*, **44,** Elsevier, Amsterdam.